

Environmental heterogeneity patterns plant species richness and turnover in two hyperdiverse floras

Running title: Environmental heterogeneity and plant species richness

Ruan van Mazijk, Michael D. Cramer & G. Anthony Verboom

Department of Biological Sciences, University of Cape Town, Rondebosch, South Africa

Corresponding author: RVM (ruanvmazijk@gmail.com, +27 21 650 3684)

ORCID nos.: RVM: 0000-0003-2659-6909, MDC: 0000-0003-0989-3266, GAV: 0000-0002-1363-9781

Abstract

****Aim:**** To quantify the explanatory power of heterogeneity in predicting plant species richness and turnover here in the Greater Cape Floristic Region and in the Southwest Australia Floristic Region. We compare the environmental heterogeneity in each region, how species richness and turnover interact in each region to produce the observed patterns of richness, and what different forms of environmental heterogeneity better predict richness in each region. We expect the Cape to be more heterogeneous in most environmental axes, and at a finer grain, such that the consequent high levels of species turnover explain the Cape's greater species richness per unit area. We also conjecture that edaphic heterogeneity will be an important factor in predicting richness in S.W. Australia.

Location: The Greater Cape Floristic Region in southwest Africa (the Cape), and the Southwest Australia Floristic Region (SWA)

Taxon: Vascular plants

Methods: Geospatially explicit floral and environmental data, non-parametric statistics, boosted regression tree modelling

Results: The Cape is more environmentally heterogeneous and has higher levels of floristic turnover than SWA. We find that environmental heterogeneity is the main predictor of species richness in the Cape, and somewhat less so for SWA. Edaphic conditions are found to be of more biologically important in the Cape, though this is contingent on the quality of the data modelled.

Main conclusions:

Keywords: biodiversity, environmental heterogeneity, fynbos, Greater Cape Floristic Region, kwongan, macroecology, species richness, species turnover, vascular plants, Southwest Australia Floristic Region

Acknowledgements

This work was funded by the South African Department of Science and Technology (DST) and the National Research Foundation (NRF) under the DST-NRF Innovation Honours Scholarship (to RVM), and by the South African Association of Botanists (SAAB) Honours Scholarship (to RVM). Thanks go to the Department of Biological Sciences, University of Cape Town, for providing a 2TB external hard drive for local GIS data storage. Many computations were performed using facilities provided by the University of Cape Town's ICTS High Performance Computing team (hpc.uct.ac.za).

1 Introduction

Biodiversity represents the variety of living things, and the variety of ecological and evolutionary processes responsible for it (Bøhn & Amundsen, 2004). Studying the distribution of biodiversity in space is a major avenue of biological research (???, Kreft & Jetz, 2007). Regional-scale geographic patterns in species richness have long been studied, particularly in biodiversity hotspots (Cook et al., 2015). The spatial distribution of species richness can be explained in terms of the physical environment. Properties of the environment have been suggested to influence species richness in three ways: (i) productivity, water, and energy to enable organismal growth, and resources (i.e. niche space) to support a wider range of species (Gaston, 2000; Kreft & Jetz, 2007; Mouchet et al., 2015); (ii) stability, which enables species' persistence; and (iii) heterogeneity, which enables ecological speciation and possible barriers to gene flow, and with a wider variety of environments to facilitate species' co-existence (Thuiller et al., 2006; Mouchet et al., 2015; Cramer & Verboom, 2016). The physical environment, then, can be used to explain species richness in a

41 local-deterministic sense, and in a historical context (Ricklefs, 1987).

42 The maintenance of species richness, particularly the coexistence of high numbers of species in biodiversity
43 hotspots, is often regarded as “paradoxical” (Hart et al., 2017), and is a central problem in ecology (Ricklefs,
44 1987; Kreft & Jetz, 2007; Hart et al., 2017). Species richness is constrained by the ability of habitats to support
45 a variety of species—its ecological carrying capacity (Mateo et al., 2017). This is exemplified in approaches to
46 modelling species richness as a function of environmental predictors in a correlative framework
47 (“macro-ecological models”; Mateo et al., 2017). Macroecological models of species richness implicitly
48 assume that communities are saturated, following species-area and species-energy relationships, and at
49 equilibrium with the environment (Mateo et al., 2017).

50 A solution to the paradox of species coexistence is environmental heterogeneity (EH): a more heterogeneous
51 environment has a larger environmental space, and can thus facilitate co-existence between species at the scale
52 of that heterogeneity. EH can also stimulate ecological speciation, should the region be environmentally stable
53 over evolutionary time-scales. Heterogeneity in the physical environment is known to be positively associated
54 with species richness (Rensburg et al., 2002; Hart et al., 2017), and has been demonstrated to do so across
55 many taxa—e.g. Canadian butterflies (??), European vertebrates (Mouchet et al., 2015), South African birds
56 (Rensburg et al., 2002), in communities along marine continental margins (Levin et al., 2010), French scarab
57 beetles (Lobo et al., 2004), and for global terrestrial plants (Kreft & Jetz, 2007). The spatial scale of
58 heterogeneity, or “grain” of the environment, is important to consider (Hart et al., 2017), in the same way that
59 the spatial of absolute environmental conditions has also been considered (??; Baudena et al., 2015; Mouchet
60 et al., 2015). Species co-existence and biodiversity maintenance is indeed suggested to be scale-dependent
61 (Hart et al., 2017).

62 EH is often under-represented in macro-ecological models of species richness, and has recently been found to
63 explain up to ca. 95% of biome level species richness across South Africa (Cramer & Verboom, 2016). Models
64 that include EH yield better estimates of the richness of the Cape flora, as they account for the role
65 heterogeneous environments such as those in the Cape facilitate species coexistence (Thuiller et al., 2006;
66 Cramer & Verboom, 2016). Mediterranean-type terrestrial biodiversity hotspots, such as the Cape flora
67 included in the models by Cramer & Verboom (2016), present interesting study systems in which to investigate
68 the relationship between the environment and species richness. These systems exhibit far greater species
69 richness than predicted by their areas, productivities and latitudes (Cowling et al., 1996; Kreft & Jetz, 2007).
70 There are five Mediterranean biodiversity hotspots on Earth: the California Floristic Province, the

71 Mediterranean Basin, the Chilean Winter Rainfall-Valdivian Forests, the Greater Cape Floristic Region, and the
72 Southwest Australia Floristic Region (Cowling et al., 1996; Hopper & Gioia, 2004; Cook et al., 2015). These
73 ecosystems have regular fire-cycles (Cowling et al., 1996), climatic buffering, and long term stability (Kreft &
74 Jetz, 2007), shrubby, sclerophyllous flora (Hopper & Gioia, 2004). Together, they account for ca. 20% of
75 global vascular plant species, yet only ca. 5% of global land surface areas (Cowling et al., 1996). Various
76 hypotheses have been proposed to explain the high levels of plant species richness in these regions (Cook et al.,
77 2015). The species accumulation hypothesis states that the stability of these regions has allowed many species
78 to accrue. The species co-existence hypothesis states that these hotspots may facilitate greater degrees of
79 species co-existence in smaller spatial areas, due to fine-scale heterogeneity in their environments. Indeed, EH
80 has evolutionary implications too, stimulating ecological speciation across sharp environmental gradients.

81 Both the Southwest Australia Floristic Region (SWA) and the Greater Cape Floristic Region (Cape) are
82 Mediterranean-type biodiversity hotspots, particularly in terms of plant species. Where the Cape (with an area
83 of ca. 189,000 km²) is known to contain about 11,400 plant species (about 0.060 species per km²), SWA (area
84 of ca. 270,000 km²) has about 3,700 species (0.014 species per km²) (???). So, the Cape has ca. 4.3 times as
85 many species per km² as SWA. The Cape and SWA are appropriately often compared, due to the similarities
86 between their environments (e.g. oligotrophic soils, an oceanically buffered moderate climate) and their plants'
87 ecologies (Hopper & Gioia, 2004). These two regions present unique flora out of the five Mediterranean
88 systems, with high levels of endemism (Cowling et al., 1996), and many obligate fire-adapted species (Cowling
89 et al., 1996). Similarities withstanding, SWA is topographically and edaphically distinct from the Cape. The
90 former is topographically rather uniform (i.e. flat)—uniquely so among the world's five Mediterranean-climate
91 regions (Hopper & Gioia, 2004)). SWA possesses a mesoscale chronosequence dune system (Laliberte et al.,
92 2014; Cook et al., 2015), while the Cape is mountainous, topographically heterogeneous, and therefore
93 associated with a large degree of spatial climatic variability, with a fine-scale mosaic of geologies and soils
94 (Cowling et al., 1996; Cramer et al., 2014; Verboom et al., 2017).

95 Both regions have sources of edaphic heterogeneity, but at different scales. This edaphic variability may aid in
96 explaining the species richness in these regions (Beard et al., 2000; Verboom et al., 2017). EH can stimulate
97 ecological speciation, should the region be stable over evolutionary time-scales, as is likely the case in both the
98 Cape and SWA (Wardell-Johnson & Horwitz, 1996; Hopper & Gioia, 2004; Lambers et al., 2010; Cramer et al.,
99 2014; Laliberte et al., 2014; Cook et al., 2015). For the Cape, this richness is largely known to result from long
100 term climatic stability, and fine grain variation in geology and soils (Cramer et al., 2014). The question thus
101 arises whether heterogeneity is a significant contributor to SWA species richness as is likely the case in the

102 Cape. In the absence of topographic variability in SWA, it is proposed that the heterogeneity of that region is
103 due to the juxtaposition of soil types (Laliberte et al., 2014; Cook et al., 2015), creating extreme edaphic
104 variation.

105 **1.1 Hypothesis-v1**

106 Our main hypothesis is that the greater abiotic heterogeneity in the Cape, and the finer grain of that
107 heterogeneity, compared to that of the SWA, accounts for the Cape's greater species richness per unit area. We
108 expect the relationships between EH, species richness, and species turnover in these two regions to demonstrate
109 this. As stated above, heterogeneous environments can (i) support diverse species assemblages, and (ii)
110 stimulate ecological speciation. Thus, we expect species richness to covary with heterogeneity. Additionally, as
111 one moves across a heterogeneous landscape, we expect to find greater turnover in community composition, as
112 different environments support different species. Thus, areas of greater turnover should also be more rich, due
113 to potential complementarity between neighbouring communities increasing total richness. Consequently, we
114 expect that EH positively influences species richness and species turnover, and that species turnover itself
115 positively influences species richness.

116 **1.2 Hypothesis-v2**

117 Aim: This study investigates the role EH plays in explaining vascular plant species richness in the Cape and
118 SWA. We compare the relative importance of heterogeneity between the two regions, as heterogeneity has the
119 evolutionary role of facilitating speciation, and the ecological role of supporting diverse species assemblages.
120 Spatial scale of that heterogeneity is also considered, as the heterogeneity-richness relationship can vary with
121 habitat grain-size.

122 Our hypotheses concern the Cape and SWA's environments and floras. Our main hypothesis is that the Cape
123 possesses greater abiotic heterogeneity, and at finer grain, compared to SWA, such as to explain the Cape's
124 greater species richness per unit area, and proposed greater levels of species turnover between areas. We also
125 conjecture that the heterogeneity that predicts species richness in SWA will be more pronounced in terms of
126 edaphic variables. Here we attempt to assess six key predictions of this hypothesis, additionally investigating a
127 seventh prediction to test the conjectured role of edaphic heterogeneity in SWA. Dealing with the two regions'
128 environments, we assess (i) whether the Cape environment is more heterogeneous than that of SWA and (ii)

129 whether the Cape environment has more pronounced heterogeneity at finer scales than that of SWA. Dealing
130 with the distribution of species in the two regions, we assess (iii) whether the Cape exhibits greater levels of
131 species turnover between areas. Relating each regions' environment and flora, we finally assess (iv) whether
132 species richness and species turnover are adequately predicted by EH in both regions and whether (v) Species
133 richness and species turnover are better predicted by different forms of EH in either region (e.g. the importance
134 of edaphic heterogeneity in SWA).

135 ...

136 We employ classical statistical methods to analyse publicly available geospatial and species occurrence
137 datasets.

138 ...

139 Species distribution models (SDMs), or environmental niche models, are sets of empirical methods that relate
140 observed species presences (or similar data) to environmental and spatial variables, often correlatively (Guisan
141 & Thuiller, 2005). As SDMs rely chiefly on correlating observed species ranges with the conditions thereof,
142 they provide only a model of the realised niche of a species (Raes, 2012), which can cause issues when
143 attempting to predict responses of species to changing climate. Other assumptions of typical SDMs include that
144 the range of species considered is in equilibrium with the environment (Altwegg et al., 2014; Guisan & Thuiller,
145 2005; Hannah et al., 2005), thus limiting the efficacy of these models on dynamically ranged or highly vagile
146 species (Hannah et al., 2007). Regardless, given the dynamic nature of biotic ranges under climate change,
147 SDMs are a valuable tool in identifying the contemporary risks posed to global and regional biodiversity.

148 The GCFR is a megadiverse terrestrial biogeographic region, with high levels of endemism. Midgley et al.
149 (2003) investigated the responses the now defunct Cape Floristic Region (CFR) flora to climate change. Using
150 bioclimatic envelope models (a form of SDM), they modelled the Fynbos Biome's distribution as a whole, and
151 select Cape-endemic Proteaceae species' distributions, under current and future climate (climate scenario
152 HadCM2), and again with the impact of land use change. Their Fynbos model was an indicator of regional
153 priority for species level modelling efforts, showing a general southwards contraction of the biome. Their
154 specific Proteaceae models yielded various results: complete extinctions for some species, range contractions
155 for most, improbable range shifts in some, and range expansions in few. The range shifts predicted therein were
156 acknowledged to be improbable, due to the unmodelled limitations of plant dispersal and edaphic dependence.
157 Midgley et al. (2003) concluded that climate change is likely to have severely negative for the CFR flora.

158 However, as will be outlined below, their methods may be overpredicting losses due to climate change.

159 ...

160 The last 20 years have seen much ecological research interest in and development of SDMs, using many
161 statistical and machine-learning-based methodologies (Altwegg et al., 2014; Elith et al., 2008, 2011; Guisan &
162 Thuiller, 2005). Machine-learning-based methods in SDMs include MaxEnt (Elith et al., 2011), genetic
163 algorithms, and adaptive neural networks (Hannah et al., 2005). The use of more advanced statistics
164 (e.g. Bayesian frameworks, ordination methods (Hannah et al., 2005)) is also seen. These two avenues of
165 research have intersected in the development of boosted regression trees (BRTs) (originally “gradient boosting
166 machine”; Friedman, 1999) a system of recursively generated, non-linear regression trees, as outlined by Elith
167 et al. (2008). BRTs have been used as SDMs in southern Africa before (e.g. Thuiller et al., 2006), sometimes
168 for conservation purposes (e.g. Coetzee et al., 2009), but BRTs have yet to be used specifically to assess the
169 responses of the regional flora to climate change. BRTs have more flexibility in their predictions than more
170 traditional methods (e.g. GAMs), as they are non-linear and machine-learning-based (Elith et al., 2008).

171 ...

172 **2 Materials and methods**

173 **2.1 Overview**

174 Our analyses defined boundaries for each region, those regions’ environmental data and geospatially-explicit
175 vascular plant occurrence records, all based on publicly available data. The environmental variables chosen
176 (Table 1) for this study were intended to cover a reasonable spread of climatic, edaphic, and ecologically
177 relevant environmental axes, and are not intended to be exhaustive. We selected variables describing
178 topography (elevation), productivity (NDVI), soil status and climate and climatic seasonality.

179 We carried out this investigation at four principal spatial scales: 0.05° x 0.05° squares (the finest common
180 resolution among the environmental data sources used), quarter degree squares (QDS) (Larsen et al., 2009),
181 half degree squares (HDS) (Larsen et al., 2009) and three-quarter degree squares (3QDS). For the Cape, most
182 plant occurrence records are only accurate to QDS level. Thus, analyses involving species occurrence data were
183 necessarily limited to scales including and above QDS.

Analyses were performed in R v3.4.0–3.5.1 (R Core Team, 2018). Version-numbers of specific R packages used are presented in the bibliography.

2.2 Environmental data sources

The GCFR was treated as the areas occupied by the Succulent Karoo and Fynbos biomes in the current delineation of South Africa’s biome boundaries (Mucina & Rutherford, 2006). The SWAFR was treated as the areas occupied by the Southwest Australia savanna, Swan Coastal Plain Scrub and Woodlands, Jarrah-Karri forest and shrublands, Southwest Australia woodlands, Esperance mallee, and Coolgardie woodlands in the World Wildlife Fund Terrestrial Ecoregions dataset (Olson et al., 2001) in order to closely match the currently delineated SWAFR (Gioia & Hopper, 2017, Hopper & Gioia (2004)). For the sake of readability, we shall refer to the GCFR and SWAFR simply as the Cape and SWA from hereon.

Geospatially-explicit raster layers were acquired for a selection of environmental variables (Table 1), for the regions of interest. Raster data were re-projected to a common coordinate reference: WGS84 (NIMA, 2000), using the “rgdal” (???) package in R (R Core Team, 2018). All data were re-sampled to 0.05° resolution using the “resample” function in the R package “raster” (???), with the “bilinear” method.

An emphasis was made on using satellite-derived environmental data in this work, in order to minimise differences in data quality and methodologies between the Cape and SWA. Additionally, satellite-derived data have been shown to benefit regional-scale species distribution models (Deblauwe et al., 2016), thus motivating their use in this regional-scale study. The environmental data used in this study were derived from NASA’s SRTM digital elevation model (Farr et al., 2007), NASA’s MODIS/Terra spectroradiometric data for land surface temperature and NDVI, the Climate Hazards Group’s CHIRPS rainfall dataset (Funk et al., 2015), and the International Soil Reference and Information Centre’s SoilGrids250m edaphic dataset (Hengl et al., 2017) (Table 1). SRTM and MODIS are entirely derived from satellite measurements, whereas CHIRPS is interpolated from weather station data with satellite-derived radiometric measurements. SoilGrids250m is a machine-learning derived product, based on soil measurements as a function of many covariates, including MODIS and STRM sources (see Hengl et al., 2017), using random-forests and other classification-tree-based methods, including gradient-boosting. For the soil data considered here (Table 1), we used depth-interval weighted average values as the value for a particular soil variable in a given place.

Climatic and spectral data arise from satellites monitoring properties of the Earth’s surface through time. We

212 therefore use the mean annual values for rainfall, surface temperature, and NDVI in each pixel in our analyses.
213 Pronounced seasonality of rainfall is a known feature of mediterranean systems (???). We describe this
214 seasonality by computing computing the precipitation in the driest quarter (PDQ), using methods based on the
215 “biovars” function in the R package “dismo”.

216 **2.3 Plant occurrence data**

217 Geospatially-explicit records of vascular plant occurrences were downloaded from the Global Biodiversity
218 Information Facility (GBIF, Table 1). Queries were made for tracheophyte records from within the borders of
219 the Cape and SWA as treated here (GBIF, 24 July 2017, GBIF (24 July 2017)). Only records with defined
220 species and intra-specific ranks were kept. Intra-specific occurrences were treated as simply being
221 representative of their species. This resulted in FIXME unique species names in the Cape, and FIXME in SWA.

222 We cleaned these data using the R package “taxise” (???, (???)) to check that these species names had
223 accepted-status among taxonomic databases. We queried two major taxonomic databases: the Global Name
224 Resolver (GNR), and the Taxonomic Name Resolution Service (TNRS). Should either one of these services
225 return at least one match for a given name, then that name was accepted. Those names for which no full
226 binomial matches were found in either database were excluded from the final list of species. The number of
227 species names excluded totalled at FIXME and FIXME for the Cape and SWA respectively. Especially for
228 SWA, these numbers may be deemed appreciably high. But, the occurrence records that would be dropped, as a
229 consequence of these names’ removals, appeared randomly distributed in geographic space in both regions. As
230 such, any effect of the loss of these records in this analysis is likely uniform within the two regions.

231 After the unaccepted names were removed, it was important to ensure that a species was not listed under
232 multiple synonyms. Such cases would skew estimates of species richness and turnover in this study. In light of
233 this, the remaining names were queried in the Tropicos and Integrated Taxonomic Information System (ITIS)
234 databases for their known synonyms, again using “taxize”. These were collated to produce a nomenclatural
235 “thesaurus” for the Cape and SWA species. This consisted of a list of the accepted species names in a region,
236 each associated with a list of known synonyms. We amended species’ names in the GBIF occurrence data, in
237 order ensure species were listed under only one of these synonyms, replacing all appearances of a species’
238 synonyms with the first synonym used in the list.

239 Lastly, We removed any species from both regions that are invasive aliens or non-indigenous. Alien species

240 lists for plants in South Africa and Australia were acquired from the IUCN’s Global Invasive Species Database
241 (<http://www.iucngisd.org/gisd/>).

242 The final total plant species richness in each region was FIXME and FIXME for the Cape and SWA
243 respectively. These final collections of species occurrence records were converted to raster-layers, wherein
244 pixel-values represented the species richness of vascular plants within that pixel. These rasters were produced
245 at QDS, HDS, and 3QDS resolutions.

246 **2.4 Analyses**

247 **2.4.1 Quantifying environmental heterogeneity**

248 In order to assess predictions (i) and (ii), we needed to describe the EH in both regions. Using the R package
249 “raster” (???), we used a modified version of the “roughness” index in the “terrain” function. For a three by
250 three neighbourhood N of cells, our index of roughness R is the average square-root of the squared difference
251 between each of the n neighbour cells’ values x_i and the central focal cell’s value x_{focal} :

$$R(N) = \frac{1}{n} \sqrt{\sum_{i=1}^n (x_{\text{focal}} - x_i)^2} \quad (1)$$

252 This value, notionally equivalent to the standard deviation of values relative to the focal value, is ascribed to
253 the focal cell. Note, in order to use as much data from within regions’ borders as possible, roughness was
254 computed if a focal cell had at least one neighbour cell. Using this index, we produced raster layers of each of
255 our nine environmental variable’s heterogeneity. We compared the distributions of “roughness” values in each
256 variable in each region with non-parametric Mann-Whitney U -tests, as almost all variables were highly
257 non-normal, and could not be normalised by log-transformations. We also compare the effect size of the Cape
258 vs SWA using the “common language effect size” ($CLES$), using the R package “canprot”. The $CLES$ is the
259 proportion of all pairwise comparisons between two sample groups’ observations where one group’s value is
260 greater than the other’s. We calculated the $CLES$ as the proportion of pairs where Cape roughness values
261 were greater than that of SWA. This allowed us to assess prediction (i). To compare the spatial scales of
262 heterogeneity (prediction (ii)) between each region, we repeated this analysis at all four spatial scales. This
263 entailed recalculating the roughness layer for each variable after the original layer (0.05 degrees resolution) had
264 been rescaled to each of the coarser resolutions.

265 2.4.2 Quantifying species turnover

266 Regarding prediction (iii), we wished to compare the general degree of species turnover in each region. To
267 compare the extent of species turnover between the Cape and SWA, we determined two metrics of species
268 turnover. The first, computes the mean species turnover as Jaccard distances (???) between each pair of QDS
269 within each HDS (\bar{J}_{QDS} , based on HDS with $2 \leq n \leq 4$ QDS) in both regions. The second is defined in terms
270 of Whittaker's additive definition of β -diversity (???), as follows:

$$\gamma = \alpha + \beta \quad (2)$$

271 Here, we treat species richness at the HDS-scale (S_{HDS}) as γ -diversity and at the QDS-scale (\bar{S}_{QDS}) as
272 α -diversity. Intuitively, the species richness of an area is the result of some combination of the richness of sites
273 within that area and the difference in species complements between those sites. Thus, we partition γ -diversity
274 as in Equation (2), such that β -diversity is the difference between γ - and α -diversity. We compare the
275 distributions of \bar{J}_{QDS} and T_{HDS} using non-parametric Mann-Whitney U -tests, in order to guard against
276 non-normality.

277 2.4.3 Predicting richness and turnover with environmental heterogeneity

278 Regarding prediction (iii), we wished to compare the general degree of species turnover in each region. For (iv)
279 and (v) we modelled species richness (S) and turnover as a function of various combinations of environmental
280 and environmental heterogeneity variables in both regions using boosted regression-tree (BRT) modelling
281 techniques. This allowed us to explore which axes of environmental heterogeneity are most influential on
282 vascular plant species richness and turnover, and the differences in the importance of such axes between the
283 Cape and SWA.

284 BRTs are a flexible machine learning-based model of response variables and do so without involving normal
285 null-hypothesis significance testing (Elith et al., 2008), and have been employed previously to model species
286 richness (Thuiller et al., 2006; see Mouchet et al., 2015; Cramer & Verboom, 2016) as macro-ecological
287 models. BRTs are developed through the iterative generation of non-linear regression trees. BRTs are an
288 ensemble-approach, in which a prediction \hat{y}_i is based on the weighted sum of the predictions of progressively
289 “less important” regression trees (t_k), as opposed to the predictions of one tree (Elith et al., 2008). For $k \rightarrow nt$

290 number of trees, where each tree is itself a function of the matrix \mathbf{X} of j predictor variables ($t_k = f(x_{ij})$), a
291 BRT-model can be represented as follows:

$$\hat{y}_i = \sum_{k=1}^{nt} w_k t_k \quad (3)$$

292 BRTs have two major meta-parameters over which users have control (???): the learning rate (lr , the rate at
293 which iterative trees reduce predictive deviance during model-training, controlling the contribution of each tree
294 to the final model) and tree complexity (tc , the number of nodes on a given regression-tree, i.e. the maximum
295 interaction depth the model is permitted to fit).

296 BRTs were implemented here to predict both vascular plant species richness and turnover in each HDS, as a
297 function of environmental variables and environmental roughness values in those cells, as Gaussian responses,
298 thus resulting in two BRT-models for each region. We treated richness as S_{HDS} and turnover as \bar{J}_{QDS} . The
299 natural logarithm of species richness was used, in order to satisfy the assumptions of a Gaussian response.
300 Note, this is not strictly because BRTs have any parametric assumptions concerning the distribution of the
301 response variable, but rather to aid in applying the Gaussian-family of BRT algorithms to the richness data
302 available. Additionally, BRTs were implemented to predict vascular plant species richness at the QDS-scale
303 (S_{QDS}), thus resulting in a total of six BRT-models presented here.

304 As recommended by Elith et al. (2008), BRT models were trained on a set of non-collinear predictor variables
305 using “gbm.step” in “dismo” (???) and “gbm” (???). Collinear predictor variables can skew the interpretation
306 of results, as the relative influence of mutually collinear variables is reduced. Collinearity among the nine
307 environmental predictor variables and their respective nine roughness-equivalents was assessed using
308 “removeCollinearity” in the R package “virtualspecies” (???) separately for each region, such that variables
309 were no more than 80% collinear (Pearson’s $r \geq 0.80$). When faced with a cluster of collinear variables, one
310 variable was chosen manually therefrom. Where possible, the roughness-equivalent of an environmental
311 variable was included if its absolute-equivalent could also be included. When interpreting the results of BRTs,
312 it is important to consider the effects of the variables included as representative of the effect of the excluded
313 variables with which it was found to be collinear.

314 In order to select ideal lr and tc all models (described below) were trained on the final non-collinear predictor
315 sets iteratively for 25 combinations of a range of tc values (1 to 5) and a range of lr values (0.01, 0.005, 0.001,
316 5×10^{-4} , 1×10^{-4}). The function “gbm.step” optimises the number of trees (nt) using cross-validation during

model training (Elith et al., 2008) by halting iteration when predictions begin to overfit. For all models, we used 10 cross-validation folds (i.e. use 10 different randomly selected training data sets), a tolerance-threshold of 0.001, a bagging-fraction of 0.75 (proportion of training data randomly chosen to generate each tree), and trained models starting with 50 trees, with each iterative step adding 50 trees at a time, up to a maximum of 10,000 trees. Following this iterative parameter optimisation, Gaussian BRT models were constructed with $tc = 3$ and $lr = 0.001$, along with the other settings described.

The optimum configuration of lr and tc for the final model is a trade-off between model fit (e.g. pseudo- R^2 ; Equation (4)) and complexity (nt). A tc of 5 was chosen for the final model. This follows the recommendations of Elith et al. (2008), where lr and tc are advised to be adjusted inversely. This was chosen in order to account for the complex interactions determining species richness. To avoid overfitting, an intermediate lr of 0.001 was chosen.

2.4.4 Assessing BRT-predictions' fit

BRT-model performance can be described by measuring the variance in a dataset a BRT-model has explained, quantified here by R^2_{pseudo} , which is the proportion of null deviance D_{null} explained by some model i . Formally, it is defined as follows:

$$R^2_{\text{pseudo}} = 1 - \frac{D_i}{D_{\text{null}}} \quad (4)$$

The derivation of this metric is not easy to interpret, as it is not immediately clear what model deviance is. Alternatively, comparing expected (i.e. model-predicted) and observed data has more heuristic appeal. We employed this metric of BRT-model performance too. We regressed expected against observed richness and turnover, and calculated the R^2 -value for those regressions (hereafter $R^2_{\text{E-O}}$).

The BRT-model fitting algorithm contains intrinsic stochasticity, due to the random partitions made in a dataset during cross-validation. Though this randomness is usually negligible (e.g. variables' contributions vary from run-to-run by a few decimal places), we reran each of the six BRT-models (see above) 1000 times in order to account for this stochasticity. Where indicated, we either present the averages of these replicate-models' results or the results of a representative model from each set of replicates.

In order to assess the reliability of the conclusions drawn from these models, we randomly permuted the

response data (S_{QDS} , S_{HDS} and \bar{J}_{QDS}) with respect to the environmental and heterogeneity data, and reran all six BRT-models 999 times (with the final non-collinear predictor sets and preconfigurations above). This also allows us to remove any effect of spatial autocorrelation in generating the observed correlations between patterns of species occurrence and environment (???), and to allow us to assess the significance of our results relative to a random null. For all six models, the majority of the 999 permuted models failed to find associations between the response and predictor variables. The results of those that succeeded to fit a model to completion (usually ca. 200 out of 999) are presented. The replicate and permuted BRT-models were compared using various measures of model performance (above; nt , R^2_{pseudo} (Equation (4)), R^2_{E-O}) and the ranks of these values for each replicate BRT-model relative to the 999 permuted models for that region/scope.

3 Results

3.1 Describing environmental heterogeneity across scales

Across all variables considered, the Cape is more environmentally heterogeneous in the majority of pairwise comparisons of grid-cells ($CLES > 0.50$, Mann-Whitney U -test: $P < 0.05$, Figure 1). The Cape is thus more environmentally heterogeneous than SWA overall, but the degree to which it is more heterogeneous varies between environmental variables. These effects also vary somewhat with the spatial scale concerned. In some variables, the differentiation between Cape and SWA heterogeneity lessens at coarser scales (Figure 1b). Indeed, when comparing the overall ranking and medians of Cape vs SWA roughness values for each variable, we only find non-significant differences at the coarser 3QDS scale (Mann-Whitney U tests, $P > 0.05$, Figure 1b).

Most obviously, and as expected, topographic heterogeneity is greatest in the Cape (Figure 1). Though SWA has a slightly wider distribution of elevational roughness values at coarse scales (e.g. 3QDS) compared to fine scales (0.05°), so does the Cape. As such, the relative difference in heterogeneity between the two regions seems invariant with spatial scale ($CLES \approx 0.95$, Figure 1b). This concurs with our expectations, as the Cape is mountainous and known to have steep elevational gradients (???), while SWA is much more topographically uniform. Intuitively, then, elevation serves as a “benchmark test” for our comparisons of EH here, as it is well known and expected that the Cape should be more elevationally heterogeneous than SWA.

Climatic heterogeneity is less differentiated between the Cape and SWA than elevational roughness (Figure 1a),

369 though still the Cape is indeed more climatically heterogeneous (Figure ??b). Notably, the difference between
370 Cape and SWA mean annual rainfall and land surface temperature heterogeneities is less pronounced when
371 considered at coarse spatial scales (3QDS scale, Figure ??b). Rainfall seasonality (PDQ), however, is similarly
372 more heterogeneous in the Cape across all spatial scales considered.

373 Biological productivity, as measured by NDVI, varies spatially to a similar extent in the Cape and SWA (i.e. is
374 more similarly heterogeneous, $CLES < 0.60$, Figure 1).

375 Concerning edaphic variables, the Cape and SWA are similarly heterogeneous at coarser scales, particularly in
376 terms of CEC and Soil C ($CLES \approx 0.50$, Figure 1b).

377 3.2 Comparing species turnover in the two regions

378 Following calculations of \bar{J}_{QDS} and T_{HDS} for each HDS-cell in each region, we used non-parametric
379 Mann-Whitney U -tests to compare the distributions of values in the Cape and SWA. The Cape possesses
380 generally greater floristic turnover than SWA, for both measures of turnover defined here ($P < 0.0001$, Figure
381 2a,b). Being derived from Jaccard distances, \bar{J}_{QDS} measures the average pairwise proportional floristic
382 turnover between QDS in each HDS. T_{HDS} , however, represents the β component of γ -diversity. As
383 γ -diversity (S_{HDS}) in the Cape is more greatly a function of β -diversity (T_{HDS}) than in SWA, the
384 complement is necessarily true: γ -diversity in the Cape is less a function of α -diversity (\bar{S}_{QDS}) than in SWA.

385 3.3 Predicting richness and turnover with environmental heterogeneity

386 Vascular plant species richness and turnover are found to both be predicted primarily by environmental
387 heterogeneity in the Cape (Figure 3a–c) and at least in-part by environmental heterogeneity in SWA (Figure
388 3d–f). Our six BRT-models performed adequately, and detected relationships between patterns of species
389 occurrence and the environment that do not occur in the permuted datasets (Figures 4 and 3, Table 2).

390 BRT-models of species richness at the QDS-scale in each region seemed to generally performed best, as these
391 models had generally fit the greatest number of trees (nt , Figure 4a), and higher R^2 -values (Figure 4b,c).
392 Notably, SWA models of species richness and turnover at the HDS-scale out-performed Cape models, while at
393 the QDS-scale the Cape models performed as-well or better (Figure 4, Table 3).

394 Across our BRT-models of species richness and turnover, the sets of environmental variables important to

model predictions differ substantially between the Cape and SWA, both in terms of which aspects of the environment were found to be biologically relevant and in terms of the relative importance of absolute and heterogeneity variables (Figure 3). Most obviously, species richness and turnover in the Cape are predicted in majority by environmental heterogeneity, which is not the case in SWA (piecharts inset Figure 3). Species richness and turnover in the Cape are predicted by a broad suite of environmental variables, with no individual variable contributing more than ca. 20% to any model prediction (Figure 3a–c). The SWA models' predictions, however, are largely determined by MAP (Figure 3d–f).

Species richness at QDS-scales, and to a lesser extent at HDS-scales, in the Cape is predicted in large part by edaphic conditions (Figure 3a,b). Contrastingly, richness in SWA across both scales is mostly predicted by MAP and other climatic variables (Figure 3d,e). Interestingly, topographic heterogeneity did not feature as highly in contributing to Cape predictions as we expected (Figure 3a–c).

Our BRT-models of species richness at QDS- and HDS-scales, in both regions, rank environmental variables somewhat differently (Figure 3a,b,d,e), though these differences are slightly less extreme than would be expected by chance ($P_{1-2} < 0.01$, Figure 5). This suggests a weak, but measurable, scale-dependence of the importance of different environmental variables' associations with species richness.

It is noteworthy that BRT-models of species turnover (at HDS-scales) (Figure 3c,f) rank variables similarly to models of richness at HDS-scales ($P_{2-3} \leq 0.005$, Figure 5). This is likely due to the fact that species turnover covaries with species richness. As such, though the signs of relationships determining turnover may differ from those determining richness, the importances of different variables would be similar.

4 Discussion

Conclusion: The Cape is more generally environmentally heterogeneous than the SWA, as expected (see prediction (i)). Though, there are cases where the SWA is arguably at-least-as-heterogeneous as the Cape, and we can observe here extreme regions of high edaphic heterogeneity, at fine scales, in SWA. These surpass the edaphic heterogeneity of the Cape, supporting our seventh prediction/conjecture.

We also have support for prediction (ii), as seen in Fig. ??.

I have provided support for the hypothesis that the difference in plant species richness between the GCFR and SWAFR is accounted for by the fact that the GCFR is more abiotically heterogeneous than the SWAFR. As

422 expected, the GCFR is shown to possess (i) a quantifiably more heterogeneous environment, and (ii) is
423 heterogeneous at a finer spatial scale than the SWAFR. I have shown that vascular plant species richness (iii)
424 can be explained in terms of environmental conditions, including environmental heterogeneity, in both the
425 GCFR and SWAFR. Also, I have shown that (iv) the set of environmental axes that explain plant species
426 richness, both absolute and as heterogeneity, differs between the GCFR and SWAFR. These findings contribute
427 towards an understanding of the ecological conditions that facilitate species coexistence (and likely stimulate
428 ecological speciation) in these two regions.

429 These two regions present differentiable environmental spaces, each with heterogeneity varying across spatial
430 scales. The clear separation of the regions' topographic features is as expected (Figures ??A, ??). Indeed,
431 topography seems to be the most striking distinction between the regions. The Cape region has been found
432 previously to have the second highest median topographic heterogeneity of the five Mediterranean-climate
433 regions (Bradshaw & Cowling, 2014). The GCFR has a much wider range of scales exhibited in the
434 heterogeneity across its environmental axes. Notably, each region has finer scale heterogeneity in some
435 variables, and coarser scale in others—neither region is necessarily more fine or coarse than the other, as it
436 depends on the variable concerned. BRT-models of species richness in both regions reveal species richness to
437 depend on those environmental axes that differentiate the two regions (Figures ??, ??). The importance of
438 variables is also shown to vary with spatial scale (Figure ??), as previously suggested may be the case when
439 modelling geographic patterns of biodiversity (Baudena et al., 2015). Indeed, as Cowling et al. (1996)
440 describes differing patterns of species richness across spatial scales, so do the predictors of those patterns vary
441 with scale (Hart et al., 2017).

442 The fact that a combination of absolute and roughness variables is also as predicted by the hypothesis in this
443 study. In the models developed by Cramer & Verboom (2016) for South Africa, roughness in topography was
444 largely superseded as an important predictor of species richness by other roughness variables. My models,
445 however, did not show this. Similar to the study by Rensburg et al. (2002), my models revealed roughness in
446 topography and other variables to be important. Although, Rensburg et al. (2002) considered differences
447 within pixels, as opposed to this study, which considered differences between pixels. My models, those of
448 Cramer & Verboom (2016), and those of Rensburg et al. (2002), do not all concur as to the role of roughness in
449 elevation vs. more biologically meaningful variables in explaining species richness. The source of these
450 discrepancies is unclear, though no doubt complex. The complements of environmental variables and
451 methodologies used in these studies do differ, limiting extensive comparison between these analyses.

452 The determinants of vascular plant species are shown to be region specific (Figures ??, ??, ??). The importance
 453 of MAP and roughness in rainfall seasonality (PCV) in predicting richness in the SWAFR (Figure ??I, ??J),
 454 aligns with the steep climatic gradients observed there (Cook et al., 2015). The soil variables that determine
 455 plant species richness in the model for the SWAFR (Figures ??K, ??L) differ to those that determine richness in
 456 the GCFR (Figures ??G, ??H), further highlighting the edaphic differences between these two regions.
 457 Although both are nutrient leached systems, the SWAFR is flat, with soil-chronosequences (Laliberte et al.,
 458 2014; Cook et al., 2015), while the GCFR is mountainous (Cowling et al., 1996; Cramer et al., 2014; Verboom
 459 et al., 2017). The importance of roughness in soil density, and absolute texture, in the SWAFR (Figures ??K,
 460 ??L) highlights the changes in soil that are associable with age of the substrate (e.g. particle size) as being
 461 biologically relevant to species richness. The positive effect of soil clay content on species richness in the
 462 SWAFR aligns with the findings of Laliberte et al. (2014) that richness in the SWAFR increases with soil age.

463 NDVI is more heterogeneous across the GCFR than the SWAFR (Figures ??A). The fact that thermal variables
 464 tend to be more rough in the GCFR (Figure ??A) is likely due to possible covariance of the MODIS/Terra
 465 products with topography, as MODIS data used here describes land surface temperature. As the GCFR is
 466 topographically rugged, the roughness of NDVI may arise from this. Despite this, NDVI is an integrating
 467 variable, which captures information about productivity, light availability, and soil nutrients (Power et al.,
 468 2017). The fact that absolute NDVI contributes to predicting species richness in the GCFR, especially at finer
 469 spatial scales (Figure ??E) demonstrates the role of ecological productivity in facilitating the coexistence
 470 diverse species assemblages. Environmental heterogeneity, then, is integral to explaining patterns of species
 471 richness, but must be considered along with resource- and energy-availability axes. In so much as a diverse
 472 environmental space supports more species, the materials and productivity required for biota to thrive are also
 473 needed to support species (???; Gaston, 2000; Bøhn & Amundsen, 2004; Kreft & Jetz, 2007). As such, my
 474 findings, along with those of previous studies (Rensburg et al., 2002; Thuiller et al., 2006; Kreft & Jetz, 2007;
 475 Cramer & Verboom, 2016), suggest that there is ecological and evolutionary consequence to resource
 476 availability *and* environmental heterogeneity, in that they tend to be positively associated with species richness.

477 The combined BRT-model of species richness for both regions reveals soil clay content as an important
 478 predictor, at coarse spatial scales, despite this variable not being particularly important within each region
 479 separately (Figure ??). Though this model does not strictly consider the regions as separate, this finding may
 480 indicate that the relationship between clay content and species richness differs between the regions. So far as
 481 clay content can be used to predict species richness, it matters more to those predictions when applied to large
 482 sections (i.e. coarse scales) of each regions.

483 Kreft & Jetz (2007) modelled global terrestrial vascular plant species richness, which focussed on primarily
 484 absolute environmental values, underestimated the richness of the Cape flora. Though Kreft & Jetz (2007) did
 485 include topographic heterogeneity in their predictor set, topography is often a proxy for more biologically
 486 meaningful variables (Cramer & Verboom, 2016). This explains why the inclusion of these variables
 487 (e.g. roughness in mean annual precipitation) yields more accurate predictions of species richness. Indeed,
 488 Thuiller et al. (2006) also included topographic heterogeneity. Cramer & Verboom (2016) described 68% of
 489 species richness at the QDS scale across South Africa. Regarding the GCFR, depending on whether one
 490 consults pseudo- R^2 (Table 3), the ratio of mean predicted to observed richness per grid-cell (Table 5), or the
 491 distributions of predicted vs. observed richness values per grid-cell (Figure ??), I have achieved a similarly
 492 suitable level of predictive accuracy. There is, though, still unexplained species richness in light of my models.
 493 As Cramer & Verboom (2016), Rensburg et al. (2002), Thuiller et al. (2006), and Mouchet et al. (2015) have
 494 done, these macro-ecological models are a-historical. Evolutionary considerations of species richness in
 495 geographic space are worthwhile, especially in regions with environments stable over evolutionary time.

496 The findings here are correlative. There are, however, many proposed mechanisms to explain the correlative
 497 signals demonstrated here. My findings support the hypothesis that Mediterranean systems' plant species
 498 richness is a function of spatial variability in environmental conditions. This can stimulate diversification, and
 499 maintain that diversity by providing a range of habitats for species co-existence. Oligotrophic soils can stimulate
 500 an increase in functional diversity, through the evolution of diverse nutrient acquisition strategies (Lambers et
 501 al., 2010; Verboom et al., 2017) (e.g. sclerophylly (Cramer et al., 2014; Cook et al., 2015)). An aspect of the
 502 environment I have neglected to consider is fire, shown to also contribute to predictions here in the GCFR
 503 (Cramer & Verboom, 2016). Cardillo (2012) have shown the structuring forces behind species co-occurrence
 504 patterns, and thus likely species richness, differ between species-pairs with different post-fire responses and
 505 those with similar post-fire responses.

506 Though the GCFR was correctly predicted to have, on average, more species per grid-cell at HDS and 3QDS
 507 scales than the SWAFR, this was not the case for QDS grid-cells (Table 5). This demonstrates that the GCFR is
 508 indeed overall more rich in plant species than the SWAFR, but a given HDS in the SWAFR contains fewer
 509 species than a given GCFR HDS. Thus, the greater richness in the GCFR is a product of greater turnover in
 510 species at spatial scales no more coarse than the HDS. Species turnover is an interesting aspect to species
 511 richness studies, as it species turnover is implicit to species-area and co-existence-area relationships (Hart et
 512 al., 2017). One could expect patterns of endemism and species turnover to concur with patterns in
 513 environmental heterogeneity to some degree.

514 Following from the understanding that functionally diverse assemblages, which are more likely to be more
 515 species rich, are likely to arise and/or occur in areas with diverse ecological pressures (Molina-Venegas et al.,
 516 2015), one would expect, then, heterogeneous habitats such as those in Mediterranean-type biodiversity
 517 hotspots to exhibit high levels functional beta diversity along steep environmental gradients (Molina-Venegas
 518 et al., 2015). If the niches concerning these functions are phylogenetically conserved among those biota, then
 519 one would also expect high levels of species and phylogenetic beta diversity along these gradients
 520 (Molina-Venegas et al., 2015). This concurs with the notion put forward by Power et al. (2017), wherein
 521 megadiverse systems such as these represent the results of “phylogenetic niche conservatism on a
 522 heterogeneous landscape”. Thus, species and phylogenetic turnover should covary with environmental
 523 heterogeneity in some way. Indeed, endemism, at certain scales, could also follow this pattern. Thuiller et al.
 524 (2006) demonstrated that there is phylogenetic and biome related determinants of species richness. This makes
 525 sense, in light of the difficulty of crossing biome boundaries in Mediterranean systems (Power et al., 2017).
 526 NDVI and light availability, and the heterogeneity therein, are associated with high levels of floristic turnover
 527 (Power et al., 2017). This may be indicative of ecological specialisation precluding species from crossing these
 528 boundaries, thus increasing the level of endemism within a region, while also increasing the level of turnover,
 529 and thus likely species richness, along environmental gradients. Although, this may be debated. Beard et al.
 530 (2000) state that the high levels of endemism in SWAFR are function of habitat specialisation to soil mosaics.
 531 Cf. Laliberte et al. (2014), who say that this endemism is likely due to environmental filtering along these soil
 532 turnover sequences, as opposed to the juxtaposition of specialised species along soil gradients.

533 I have demonstrated support for the idea that environmental heterogeneity is positively associated with species
 534 richness, particularly Mediterranean systems. In the SWAFR and the GCFR, high levels of endemism and
 535 biodiversity are also likely the results of long-term landscape and climatic stability (Hopper, 1979). Thus, the
 536 roles of environmental variability through space, and stability through time, are the two main ways in which the
 537 environment relates to biodiversity in these regions.

538 **Table captions**

539 Captions are also repeated alongside their respective tables for readability.

540 Table 1: Georeferenced vascular plant species occurrence and environmental data sources used in this study.
 541 Data were acquired for the Cape and SWA regions, with the temporal extent of data products used described

542 where applicable. Abbreviations are as follows: MAP, mean annual precipitation; PDQ, precipitation in the
543 driest quarter; CEC, cation exchange capacity.

544 Table 2: Average percentile-ranks for BRT-model performance measures (nt , R_{pseudo}^2 (Equation (4)), $R_{\text{E-O}}^2$)
545 of 1000 replicate BRT-models relative to 999 BRT-models fit to permuted datasets. Ranks approaching one
546 indicate that a set of replicate BRT-models had greater values than the permuted models.

547 Table 3: Estimated differences between replicate Cape and SWA BRT-models' performance measures (nt ,
548 R_{pseudo}^2 (Equation (4)), $R_{\text{E-O}}^2$) following t -tests. Positive values indicate that the Cape models had greater
549 values. In all cases, the Cape and SWA had highly significantly different values for these quality measures
550 ($P < 0.0001$).

551 **Figure captions**

552 Captions are also repeated alongside their respective figures for readability.

553 Figure 1: Types of environmental heterogeneity, compared between the the Cape and SWA—namely for (a)
554 elevation, (b) climatic variables, (c) NDVI and (d) soil variables—in each panel consisting of three sub-panels
555 per variable type. The upper row of panels shows example distributions of roughness values (Equation (1)),
556 showing the different extremes in environmental heterogeneity observed in each region when compared at fine
557 (0.05°) and coarse (3QDS) scales. Each distribution has under it an area of one. Histograms were constructed
558 using 20 breaks. In the lower row of panels, these distributions of roughness values were compared between
559 the Cape and SWA at each of the four spatial scales, not just 0.05° and 3QDS, using non-parametric
560 Mann-Whitney U -tests to test for differences. The “common language effect size” ($CLES$, see text) describes
561 these differences (b). U -tests for almost all environmental variables yielded significant differences ($P < 0.05$)
562 between Cape and SWA values (NS, non-significant differences). $CLES$ for 0.05 res. is for 5000 random cells
563 in each region, as the Mann-Whitney U -test cannot handle more than a few thousand values per sample when
564 comparing.

565 Figure 2: Species turnover, described in two forms ((a) mean Jaccard distance between QDS in each HDS
566 (\bar{J}_{QDS}), (b) additively defined turnover (T_{HDS} , Equation (2)) as a proportion of HDS richness (S_{HDS}),
567 compared between the Cape and SWA. Mann-Whitney U -tests between the Cape and SWA distributions of
568 \bar{J}_{QDS} and T_{HDS} yielded significant differences.

Figure 3: Relative influence of environmental variables (including heterogeneity variables—prefixed with “R”) in boosted regression tree (BRT) model predictions for the final six models’ response variables in Greater Cape Floristic Region (Cape) and Southwest Australia Floristic Region (SWA): vascular plant species richness at the (b,e) QDS-scale, (a,d) HDS-scale and (c,f) turnover ($= \bar{J}_{\text{QDS}}$). All BRT-models were permitted to fit three-way interactions between environmental variables. Points denote the average contribution of an environmental variable to model-predictions across the 1000 replicate BRT-models for that region/scope. Horizontal ticks denote the average for the 999 permuted BRT-models. The standard deviations above and below these means are shown with vertical lines. Note that in the case of the replicate models they are very small in most cases, obscuring them. Colour represents the general category of the environment (keyed) to which a variable belongs, as in Figure 1b. Piecharts inset display the same information (left-most piecharts), and additionally grouped according to whether a variable was absolute or roughness-transformed (right-most piecharts). F -statistics inset are for one-way ANOVAs of differences in variables’ relative influences from the replicate ($F_{\text{rep.}}$) and permuted ($F_{\text{prm.}}$) BRT-models.

Figure 4: Distributions of three measures of boosted regression tree (BRT) model performance (a) the number of trees in the model nt , (b) R^2_{pseudo} (Equation (4)), (c) $R^2_{\text{E-O}}$ (see text). These measures are presented for the six sets of permuted (pale bars) and six sets of replicate BRT-models (dark bars) as in Figure 3, coloured according to the region of interest as in Figures 1a and 2. In all cases, replicate BRT-models almost entirely out-rank the permuted models in terms of performance (Table 2) and Cape and SWA models had significantly different values for each metric (Table 3). Note, the actual differences between Cape and SWA models’ values is not realistically important in some cases.

Figure 5: Differences in the rankings of environmental variables’ (including heterogeneity variables) relative influences on boosted regression tree (BRT) model predictions of vascular plant species richness and turnover in (a) Cape and (b) SWA (as in Figure 3). Each point represents an environmental variable’s rank in BRT-model importance, decreasing in importance from left to right. Rankings used here are the same as that of the average relative influence for variables across replicate BRT-models, presented in Figure 3. Coloured lines connect points representing the same environmental variable. Points’ outlines are coloured according to the general category of the environment (keyed) to which a variable belongs, as in Figures 1b and 3, while points’ centres are coloured according to whether a variable was roughness-transformed or not. The comparisons of variables’ rankings of interest are between QDS- and HDS-scale richness (rows nos. 1 and 2) and between HDS-scale richness and turnover (rows nos. 2 and 3). Statistics (Δ - and P -values) inset at the top and bottom of each panel refer to these comparisons respectively. Δ -values represent the average absolute difference in

600 ranks across variables between two models' rankings. The associate *P*-value results from ranking the observed
 601 Δ -values against 999 Δ -values based on random permutations of variables' rankings (SI1), such that more
 602 significant *P*-values denote rankings more similar than would be expected by chance.

603 References

- 604 Baudena, M., Sánchez, A., Georg, C.-P., Ruiz-Benito, P., Rodríguez, M.Á., Zavala, M.A., & Rietkerk, M. (2015) Revealing patterns of
 605 local species richness along environmental gradients with a novel network tool. *Scientific Reports*, **5**, 11561.
- 606 Beard, J.S., Chapman, A.R., & Gioia, P. (2000) Species richness and endemism in the Western Australian flora. *Journal of*
 607 *Biogeography*, **27**, 1257–1268.
- 608 Bøhn, T. & Amundsen, P.-A. (2004) Ecological Interactions and Evolution: Forgotten Parts of Biodiversity? *BioScience*, **54**, 804.
- 609 Bradshaw, P.L. & Cowling, R.M. (2014) Landscapes, rock types, and climate of the Greater Cape Floristic Region. *Fynbos: Ecology,*
 610 *evolution and conservation of a megadiverse region* (ed. by N. Allsopp, J.F. Colville, and G.A. Verboom), pp. 26–46. Oxford
 611 University Press, Oxford.
- 612 Cardillo, M. (2012) The phylogenetic signal of species co-occurrence in high-diversity shrublands: different patterns for fire-killed and
 613 fire-resistant species. *BMC Ecology*, **12**, 21.
- 614 Cook, L.G., Hardy, N.B., & Crisp, M.D. (2015) Three explanations for biodiversity hotspots: small range size, geographical overlap
 615 and time for species accumulation. An Australian case study. *New Phytologist*, **207**, 390–400.
- 616 Cowling, R.M., Rundel, P.W., Lamont, B.B., Arroyo, M.K., & Arianoutsou, M. (1996) Plant diversity in mediterranean-climate
 617 regions. *Trends in Ecology and Evolution*, **11**, 362–366.
- 618 Cramer, M.D. & Verboom, G.A. (2016) Measures of biologically relevant environmental heterogeneity improve prediction of regional
 619 plant species richness. *Journal of Biogeography*, 1–13.
- 620 Cramer, M.D., West, A.G., Power, S.C., Skelton, R., & Stock, W.D. (2014) Plant ecophysiological diversity. *Fynbos: Ecology,*
 621 *evolution and conservation of a megadiverse region* pp. 248–272. Oxford University Press, Oxford.
- 622 Deblauwe, V., Droissart, V., Bose, R., Sonké, B., Blach-Overgaard, A., Svenning, J.C., Wieringa, J.J., Ramesh, B.R., Stévant, T., &
 623 Couvreur, T.L.P. (2016) Remotely sensed temperature and precipitation data improve species distribution modelling in the
 624 tropics. *Global Ecology and Biogeography*, **25**, 443–454.
- 625 Elith, J., Leathwick, J.R., & Hastie, T. (2008) A working guide to boosted regression trees. *Journal of Animal Ecology*, **77**, 802–813.
- 626 Farr, T., Rosen, P., Caro, E., Crippen, R., Duren, R., Hensley, S., Kobrick, M., Paller, M., Rodriguez, E., Roth, L., Seal, D., Shaffer, S.,
 627 Shimada, J., Umland, J., Werner, M., Oskin, M., Burbank, D., & Alsdorf, D. (2007) The shuttle radar topography mission.

- 628 *Reviews of Geophysics*, **45**, 1–33.
- 629 Funk, C.C., Peterson, P.J., Landsfeld, M., Pedreros, D.H., Verdin, J., Shukla, S., Husak, G., Rowland, J.D., Harrison, L., Hoell, A., &
630 Michaelson, J. (2015) The climate hazards infrared precipitation with stations—a new environmental record for monitoring
631 extremes. *Scientific Data*, **2**, 150066.
- 632 Gaston, K.J. (2000) Global patterns in biodiversity. *Nature*, **405**, 220–227.
- 633 GBIF (24 July 2017) GBIF Occurrence Download..
- 634 GBIF (24 July 2017) GBIF Occurrence Download..
- 635 Gioia, P. & Hopper, S.D. (2017) A new phytogeographic map for the Southwest Australian Floristic Region after an exceptional decade
636 of collection and discovery. *Botanical Journal of the Linnean Society*, **184**, 1–15.
- 637 Hart, S.P., Usinowicz, J., & Levine, J.M. (2017) The spatial scales of species coexistence. *Nature Ecology & Evolution*, **1**, 1066–1073.
- 638 Hengl, T., Mendes de Jesus, J., Heuvelink, G.B.M., Ruiperez Gonzalez, M., Kilibarda, M., Blagoti?, A., Shangguan, W., Wright, M.N.,
639 Geng, X., Bauer-Marschallinger, B., Guevara, M.A., Vargas, R., MacMillan, R.A., Batjes, N.H., Leenaars, J.G.B., Ribeiro, E.,
640 Wheeler, I., Mantel, S., & Kempen, B. (2017) SoilGrids250m: Global gridded soil information based on machine learning.
641 *PLoS ONE*, **12**, e0169748.
- 642 Hopper, S.D. (1979) Biogeographical Aspects of Speciation in the Southwest Australian Flora. *Annual Review of Ecology and*
643 *Systematics*, **10**, 399–422.
- 644 Hopper, S.D. & Gioia, P. (2004) The Southwest Australian Floristic Region: Evolution and Conservation of a Global Hot Spot of
645 Biodiversity. *Annual Review of Ecology, Evolution, and Systematics*, **35**, 623–650.
- 646 Kreft, H. & Jetz, W. (2007) Global patterns and determinants of vascular plant diversity. *Proceedings of the National Academy of*
647 *Sciences*, **104**, 5925–5930.
- 648 Laliberte, E., Zemunik, G., & Turner, B.L. (2014) Environmental filtering explains variation in plant diversity along resource gradients.
649 *Science*, **345**, 1602–1605.
- 650 Lambers, H., Brundrett, M.C., Raven, J.A., & Hopper, S.D. (2010) Plant mineral nutrition in ancient landscapes: high plant species
651 diversity on infertile soils is linked to functional diversity for nutritional strategies. *Plant and Soil*, **334**, 11–31.
- 652 Larsen, R., Holmern, T., Prager, S.D., Maliti, H., & Røskaft, E. (2009) Using the extended quarter degree grid cell system to unify
653 mapping and sharing of biodiversity data. *African Journal of Ecology*, **47**, 382–392.
- 654 Levin, L.A., Sibuet, M., Gooday, A.J., Smith, C.R., & Vanreusel, A. (2010) The roles of habitat heterogeneity in generating and
655 maintaining biodiversity on continental margins: an introduction. *Marine Ecology*, **31**, 1–5.
- 656 Lobo, J.M., Jay-robert, P., Lumaret, J.-p., Lobo, J.M., Jay-robert, P., & Lumaret, J.-p. (2004) Modelling the Species Richness

- 657 Distribution for French Aphodiidae (Coleoptera, Scarabaeoidea). *Ecography*, **27**, 145–156.
- 658 Mateo, R.G., Mokany, K., & Guisan, A. (2017) Biodiversity Models: What If Unsaturation Is the Rule? *Trends in Ecology &*
659 *Evolution*, **32**, 556–566.
- 660 Molina-Venegas, R., Aparicio, A., Slingsby, J.A., Lavergne, S., & Arroyo, J. (2015) Investigating the evolutionary assembly of a
661 Mediterranean biodiversity hotspot: Deep phylogenetic signal in the distribution of eudicots across elevational belts. *Journal*
662 *of Biogeography*, **42**, 507–518.
- 663 Mouchet, M., Levers, C., Zupan, L., Kuemmerle, T., Plutzar, C., Erb, K., Lavorel, S., Thuiller, W., & Haberl, H. (2015) Testing the
664 effectiveness of environmental variables to explain European terrestrial vertebrate species richness across biogeographical
665 scales. *PLoS ONE*, **10**, 1–16.
- 666 Mucina, L. & Rutherford, M.C. (2006) *The vegetation of South Africa, Lesotho and Swaziland*. South African National Biodiversity
667 Institute,
- 668 NIMA (2000) Amendment 1. 3 January 2000. Department of Defense World Geodetic System 1984. Its Definition and Relationships
669 with Local Geodetic Systems. 1–3.
- 670 Olson, D.M., Dinerstein, E., Wikramanayake, E.D., Burgess, N.D., Powell, G.V.N., Underwood, E.C., D'amico, J.A., Itoua, I., Strand,
671 H.E., Morrison, J.C., & Others (2001) Terrestrial Ecoregions of the World: A New Map of Life on Earth: A new global map of
672 terrestrial ecoregions provides an innovative tool for conserving biodiversity. *BioScience*, **51**, 933–938.
- 673 Power, S.C., Verboom, G.A., Bond, W.J., & Cramer, M.D. (2017) Environmental correlates of biome-level floristic turnover in South
674 Africa. *Journal of Biogeography*, **44**, 1745–1757.
- 675 R Core Team (2018) *R: A Language and Environment for Statistical Computing. Version 3.5.0*. R Foundation for Statistical
676 Computing, Vienna, Austria.
- 677 Rensburg, B.J. van, Chown, S.L., & Gaston, K.J. (2002) Species Richness, Environmental Correlates, and Spatial Scale: A Test Using
678 South African Birds. *The American Naturalist*, **159**, 566–577.
- 679 Ricklefs, R.E. (1987) Community diversity: relative roles of local and regional processes. *Science, New Series*, **235**, 167–171.
- 680 Thuiller, W., Midgley, G.F., Rouget, M., Cowling, R.M., F. Midgley, G., Rougeti, M., & M. Cowling, R. (2006) Predicting patterns of
681 plant species richness in megadiverse South Africa. *Ecography*, **29**, 733–744.
- 682 Verboom, G.A., Stock, W.D., & Cramer, M.D. (2017) Specialization to extremely low-nutrient soils limits the nutritional adaptability
683 of plant lineages. *The American Naturalist*, **In press**.
- 684 Wardell-Johnson, G. & Horwitz, P. (1996) Conserving biodiversity and the recognition of heterogeneity in ancient landscapes: a case
685 study from south-western Australia. *Forest Ecology and Management*, **85**, 219–238.

686 **Biosketches**

687 **Ruan van Mazijk** is currently a Masters student at the University of Cape Town, interested in phylogenetic
688 systematics, macroecology, community and functional ecology.

689 **Michael D. Cramer**

690 **G. Anthony Verboom**

691 **Author contributions**

692 MDC and GAV conceived the study question, which RVM investigated under their supervision for his BSc
693 Hons project. The analyses and programming work were largely devised by RVM, with input from the other
694 authors, and was carried out by RVM. RVM wrote the first draft of the manuscript and all authors contributed
695 equally thereafter.

Table 1: Georeferenced vascular plant species occurrence and environmental data sources used in this study. Data were acquired for the Cape and SWA regions, with the temporal extent of data products used described where applicable. Abbreviations are as follows: MAP, mean annual precipitation; PDQ, precipitation in the driest quarter; CEC, cation exchange capacity.

Variable	Source	Temporal extent	Citation
Plant species occurrences	GBIF	TODO	??, ??
Elevation	SRTM v2.0		??
NDVI	MODIS (MOD13C2)	Feb. 2000 to Apr. 2017	??
Climatic variables			
Surface temperature	MODIS (MOD11C3)	Feb. 2000 to Apr. 2017	??
MAP	CHIRPS v2.0	Jan. 1981 to Feb. 2017	??
PDQ	CHIRPS v2.0	Jan. 1981 to Feb. 2017	??
Soil variables			
CEC	SoilGrids250m (CECSOL M 250m)		??
Clay	SoilGrids250m (CLYPPT M 250m)		
Soil C	SoilGrids250m (OCDENS M 250m)		
pH	SoilGrids250m (PHIKCL M 250m)		

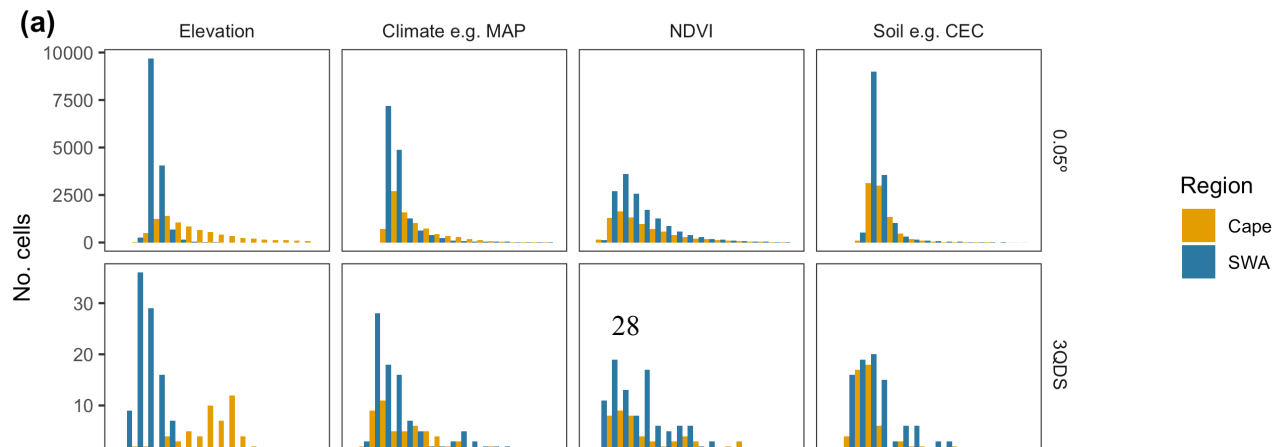
Table 2: Average percentile-ranks for BRT-model performance measures (nt , R^2_{pseudo} (Equation (4)), R^2_{E-O}) of 1000 replicate BRT-models relative to 999 BRT-models fit to permuted datasets. Ranks approaching one indicate that a set of replicate BRT-models had greater values than the permuted models.

Model	nt	R^2_{pseudo}	R^2_{E-O}
QDS-richness			
GCFR	1.000	1.000	1.000
SWAFR	1.000	1.000	1.000
HDS-richness			
GCFR	0.987	1.000	0.988
SWAFR	1.000	1.000	1.000
HDS-turnover			
GCFR	0.977	0.992	0.979
SWAFR	0.997	1.000	1.000

Table 3: Estimated differences between replicate Cape and SWA BRT-models’ performance measures (nt , R^2_{pseudo} (Equation (4)), R^2_{E-O}) following t -tests. Positive values indicate that the Cape models had greater values. In all cases, the Cape and SWA had highly significantly different values for these quality measures ($P < 0.0001$).

Model	nt	R^2_{pseudo}	R^2_{E-O}
QDS-richness	542.938	0.063	-0.005
HDS-richness	-808.994	-0.064	-0.233
HDS-turnover	-997.045	-0.052	-0.296

Figures



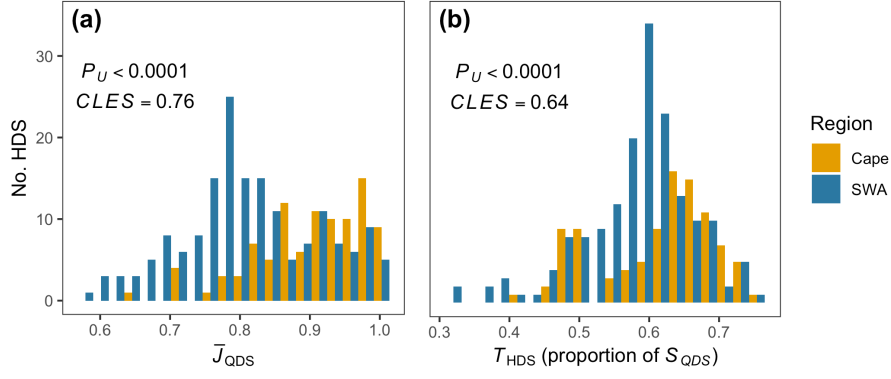


Figure 2: Species turnover, described in two forms ((a) mean Jaccard distance between QDS in each HDS (\bar{J}_{QDS}), (b) additively defined turnover (T_{HDS} , Equation (2)) as a proportion of HDS richness (S_{HDS})), compared between the Cape and SWA. Mann-Whitney U -tests between the Cape and SWA distributions of \bar{J}_{QDS} and T_{HDS} yielded significant differences.

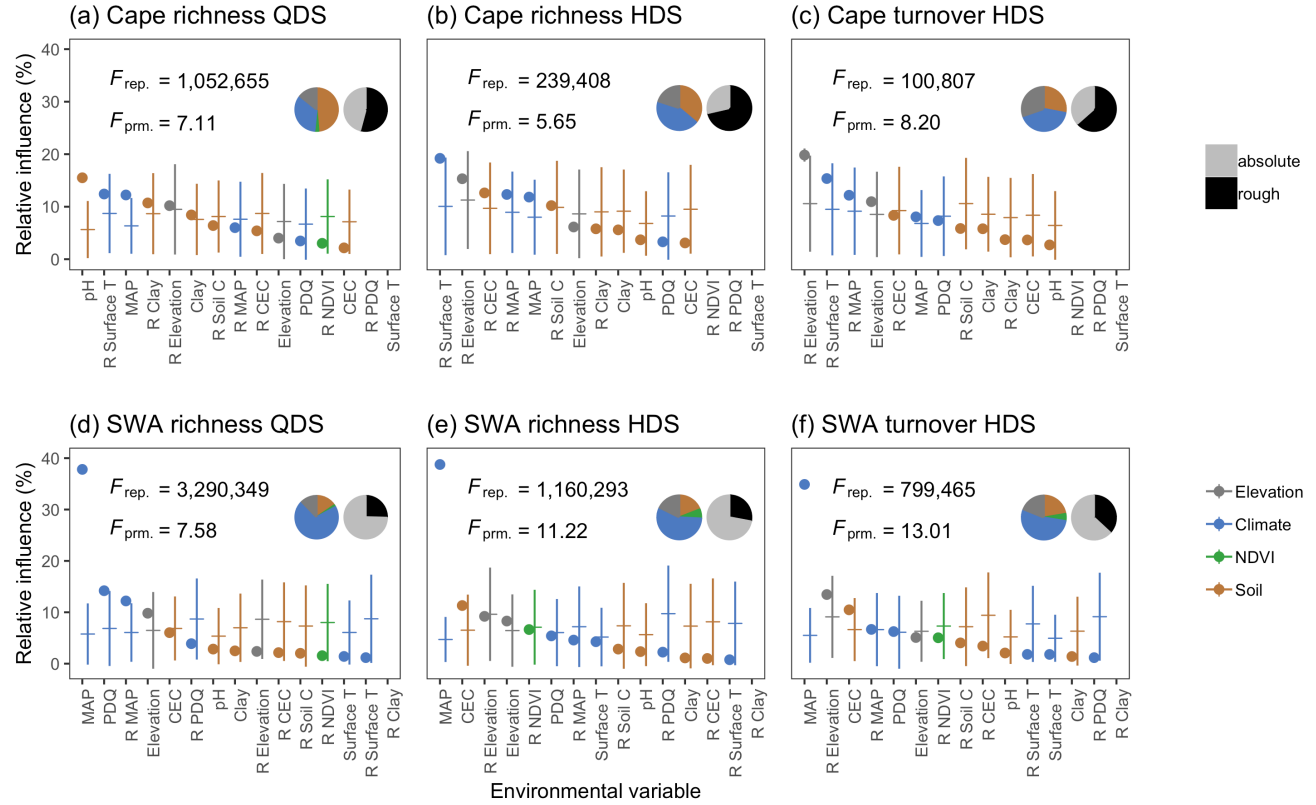


Figure 3: Relative influence of environmental variables (including heterogeneity variables—prefixed with “R”) in boosted regression tree (BRT) model predictions for the final six models’ response variables in Greater Cape Floristic Region (Cape) and Southwest Australia Floristic Region (SWA): vascular plant species richness at the (b,e) QDS-scale, (a,d) HDS-scale and (c,f) turnover ($= \bar{J}_{QDS}$). All BRT-models were permitted to fit three-way interactions between environmental variables. Points denote the average contribution of an environmental variable to model-predictions across the 1000 replicate BRT-models for that region/scope. Horizontal ticks denote the average for the 999 permuted BRT-models. The standard deviations above and below these means are shown with vertical lines. Note that in the case of the replicate models they are very small in most cases, obscuring them. Colour represents the general category of the environment (keyed) to which a variable belongs, as in Figure 1b. Piecharts inset display the same information (left-most piecharts), and additionally grouped according to whether a variable was absolute or roughness-transformed (right-most piecharts). F -statistics inset are for one-way ANOVAs of differences in variables’ relative influences from the replicate ($F_{rep.}$) and permuted ($F_{prm.}$) BRT-models.

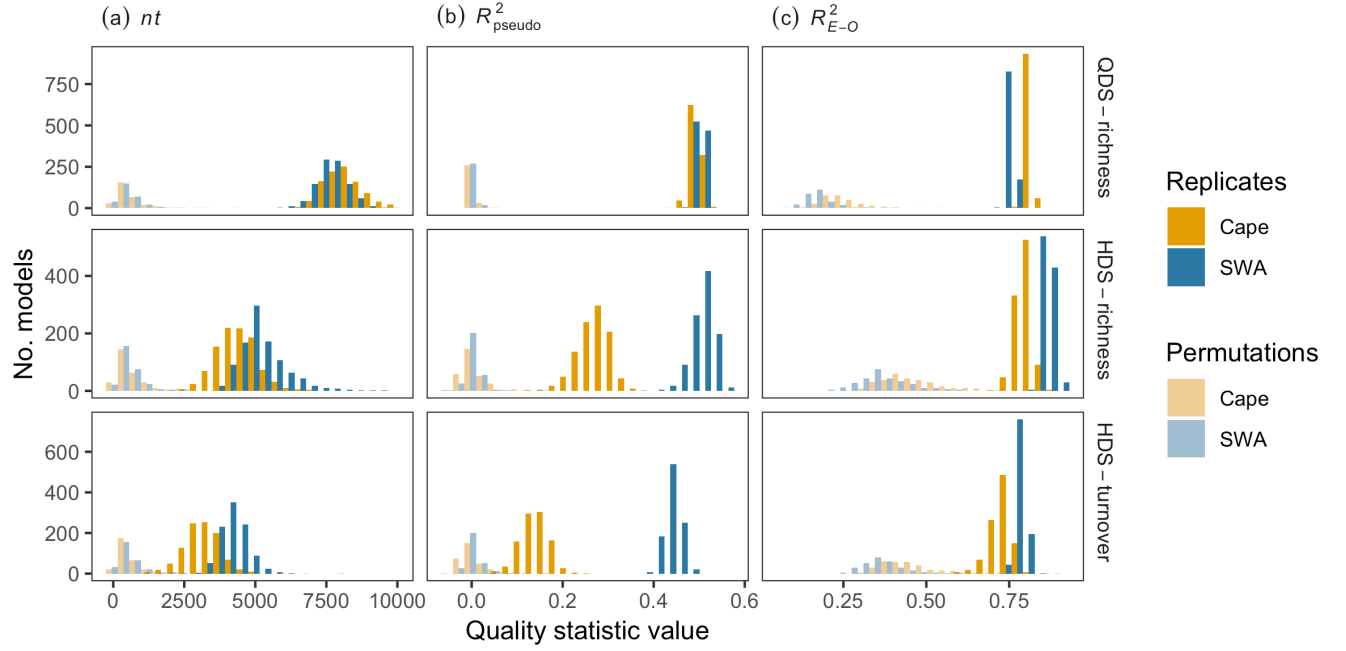


Figure 4: Distributions of three measures of boosted regression tree (BRT) model performance (a) the number of trees in the model nt , (b) R^2_{pseudo} (Equation (4)), (c) R^2_{E-O} (see text). These measures are presented for the six sets of permuted (pale bars) and six sets of replicate BRT-models (dark bars) as in Figure 3, coloured according to the region of interest as in Figures 1a and 2. In all cases, replicate BRT-models almost entirely out-rank the permuted models in terms of performance (Table 2) and Cape and SWA models had significantly different values for each metric (Table 3). Note, the actual differences between Cape and SWA models' values is not realistically important in some cases.

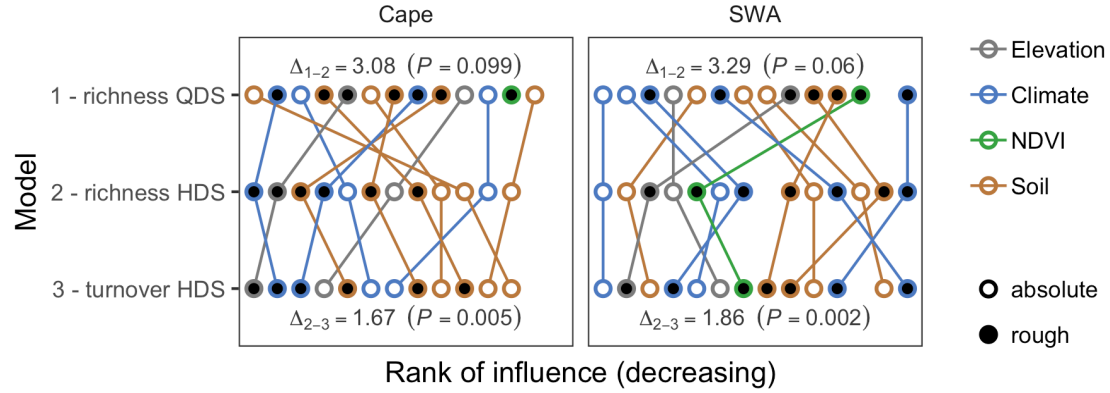


Figure 5: Differences in the rankings of environmental variables' (including heterogeneity variables) relative influences on boosted regression tree (BRT) model predictions of vascular plant species richness and turnover in (a) Cape and (b) SWA (as in Figure 3). Each point represents an environmental variable's rank in BRT-model importance, decreasing in importance from left to right. Rankings used here are the same as that of the average relative influence for variables across replicate BRT-models, presented in Figure 3. Coloured lines connect points representing the same environmental variable. Points' outlines are coloured according to the general category of the environment (keyed) to which a variable belongs, as in Figures 1b and 3, while points' centres are coloured according to whether a variable was roughness-transformed or not. The comparisons of variables' rankings of interest are between QDS- and HDS-scale richness (rows nos. 1 and 2) and between HDS-scale richness and turnover (rows nos. 2 and 3). Statistics (Δ - and P -values) inset at the top and bottom of each panel refer to these comparisons respectively. Δ -values represent the average absolute difference in ranks across variables between two models' rankings. The associate P -value results from ranking the observed Δ -values against 999 Δ -values based on random permutations of variables' rankings (SI1), such that more significant P -values denote rankings more similar than would be expected by chance.